On the estimate of the captured power by a submerged OWC through thermal measurements

L. Gurnari, F. Ruffa, M. Lugarà, G. Fulco, P. Filianoti

Abstract—**Direct measurements of water velocity is challenging, particularly for Oscillating Water Column (OWC) devices with U-ducts, as the presence of a velocity sensor can disrupt the motion field. Boccotti (2003) and Arena & Filianoti (2007) suggested an approach of assessing absorbed energy by measuring simultaneously the temperature and the pressure fluctuations of the air mass inside the plenum chamber. However, they did not provide information regarding the accuracy of the temperature sensors or the resulting estimation errors in energy flux. In this study, following that measurement technique, we examined the impact of the temperature sensor's time response on assessing changes in air volume within the chamber and, consequently, on the estimation of the energy captured by the converter. Our findings indicate that temperature measurements inside the plenum are significantly influenced by the sensor's time response, and that even recurring to forced ventilation does not guarantee satisfactory results.**

Index Terms—**U-OWC, temperature fluctuation, captured energy, thermocouple, CFD**

I. Introduction

EXTENSIVE Extensive efforts have been made in recent decades to develop and optimize technologies for renewable energy generation. The effort is focused on the one hand on the development of new energy flow management platforms that take into account the characteristics of energy production from renewable sources [1], on the other hand on the search for new energy sources, widely available and reliable. One particularly promising solution is the utilization of sea wave energy for economically sustainable electricity production [2]. Wave energy, an unlimited source, plays a crucial role in meeting renewable energy targets by converting the kinetic energy of waves into electrical energy [3]. This conversion is achieved through devices called Wave Energy Converters (WECs), which come in various types based on their working principle,installation location and wave motion orientation [4].

The Oscillating Water Column (OWC) systems utilize wave motion to generate energy and are constructed using reinforced concrete or steel structures. These systems feature a partially submerged chamber with an underwater opening that allows water to enter and compress the air in the upper part of the chamber. A turbine is capable to produce energy through the compressed air expelled [5]. When the water level recedes, air from the atmosphere enters the chamber and flows through the turbine in the opposite direction. To accommodate bidirectional airflow, low-pressure Wells turbines are commonly employed, because they don't need airflow rectification [6].

OWC systems are extensively studied for converting wave energy due to their simplicity and robustness [7]. Various OWC systems are currently being developed, with some already connected to the electricity grid, serving as demonstration applications in different countries [8]–[13]. A notable installation present in Italy concerns a system called U-OWC [14]–[19]. The U-OWC has a distinct shape that enables efficient harnessing of wave energy while preventing direct wave entry into the structure [14]. In this study, we focus on characterizing a submerged U-OWC system, which is completely submerged and consists of a caisson with a vertical inlet duct and a pressurized air cushion in the upper part of the chamber. The natural oscillation frequency of the water column varies based on the air pressure in the chamber, allowing the system to absorb energy when the frequency matches that of the waves. A turbine installed in the vertical duct is used to generate electricity [20].

To assess the feasibility of wave energy plants, it is crucial to evaluate the proportion of kinetic energy carried by the waves that can be absorbed and converted. Capture Ratio, which is the ratio of pneumatic power to the average energy flux of the incident waves, defines the hydrodynamic efficiency of an OWC system [5]. In submerged systems, where there is no exchange of air mass with the atmosphere, performance estimation requires combined measurements of pressure and velocity in the duct or chamber [14].

Various authors have proposed different experimental setups to calculate the Capture Ratio, employing different techniques to determine the energy flux into the chamber. Each setup utilizes specific sensors to measure the necessary quantities. In emerged converters, commonly used devices include wave height meters based on Doppler effect sensors, rotational systems, radar level sensors, and pressure sensors [21]–[25]. In submerged devices, pressure transducers are the most frequently employed sensors [14].

In the case of U-OWC system, is possible to evaluate

L. Gurnari, F. Ruffa, M. Lugarà and G. Fulco are with Department of Information Engineering and Sustainable Energy (DIIES) of University Mediterranea of Reggio Calabria, 89122, Reggio Calabria, Italy. (email: luana.guranri@unirc.it, filippo.ruffa@unirc.it, mariacarla.lugara@unirc.it, gaetano.fulco@unirc.it

P. Filianoti is with Department of Civil Engineering, Energy, Ambient and Materials (DICEAM) of University Mediterranea of Reggio Calabria, 89122, Reggio Calabria, Italy. (email: filianoti@unirc.it

Digital Object Identifier:
https://doi.org/10.36688/ewtec-2023-550

flux in the inlet duct to calculate water discharge into the chamber [26]. To accomplish this, speed measurements are required, using direct or indirect methods.

Direct measurement typically involves rotational systems that count revolutions and angular velocity to determine fluid velocity. In a U-OWC system, such sensors can be installed in the vertical duct, where flow velocity distribution is relatively uniform compared to the chamber with its free surface. However, introducing an obstacle in the duct can disrupt the flow, affecting measurement accuracy and plant performance. Mechanical systems are also prone to wear, breakage, and the need for periodic cleaning to remove marine vegetation from rotating parts.

An alternative emerging measurement technique involves the use of Acoustic Doppler Current Profiler (ADCP) systems to measure the absolute water speed. These systems utilize the Doppler effect, specifically the Doppler shift, to determine speed [27]. However, ADCP systems often have a bulky design, require batteries and an internal data logger, and need periodic maintenance to prevent battery depletion and the growth of algae on the transducers [8].

An approach for indirectly measuring water speed is by monitoring the instantaneous displacement of the water surface inside the chamber and deriving the velocity from it. Three commonly used sensor types for water level measurements are float meters, pressure sensors [28], and non-contact distance meters [28]–[30]. In the context of U-OWC systems, the main methods involve the use of pressure sensors or ultrasonic distance meters [18]. Non-contact sensors for water level detection offer the advantage of not being directly exposed to water, making them more resistant to erosion effects [31]. Ultrasonic devices operate by emitting ultrasonic pulses and measuring the time it takes for the receiver, often a piezoelectric transducer, to detect the reflected pulses [31], [32]. However, ultrasonic sensors need to be installed at a precise angle ($90°$) relative to the water surface to receive accurate echoes. In the presence of a sloped surface, such as inside the chamber of a U-OWC, missing echoes may occur, potentially affecting measurement accuracy. Additionally, ultrasonic sensors require frequent monitoring to ensure proper functioning and to address issues such as the formation of patinas or condensation. It is also important to account for variations in the speed of sound in air due to temperature and density changes to enhance measurement accuracy [33].

As mentioned earlier, pressure sensors are suitable for this type of application due to their fast response time, high precision, and durability. By measuring the pressure at specific points using a pair of sensors, it is possible to calculate water acceleration and integrate it to obtain velocity [34]. Unfortunately, they are too bulky to be installed in the vertical duct of a small scale U-OWC [27].

Furthermore, all the aforementioned instrumentation needs to be waterproof and is not easily miniaturizable, making it impractical for scale experiments, which are common in this research field [35]–[40].

To address these challenges, an innovative indirect measurement system is proposed in [41]. This method involves measuring thermodynamic quantities of the air mass inside the plenum, such as pressure and temperature, using commonly available sensors like pressure sensors and thermocouples. Compared to the previously mentioned methods, this approach offers several advantages. Firstly, it does not interfere with the hydrodynamics of the system, minimizing any impact on the plant's performance. Secondly, it utilizes widely accessible, robust, and cost-effective sensors. Additionally, positioning the sensors within the air chamber improves their durability as they are not in direct contact with seawater.

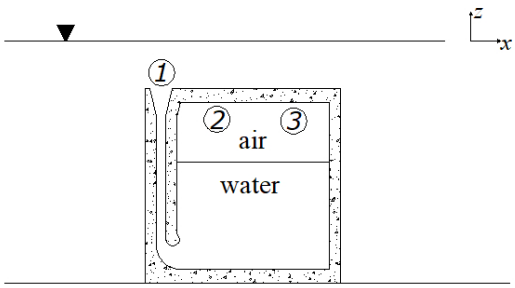

Fig. 1. Reference scheme for the positioning of the pressure transducers [①, ②] and the temperature gauge ③. The dimension of the plant is the same described in [41].

The method was initially applied to investigate the possibility of achieving strong natural resonance by tuning the mass of the air pocket inside the plant and verifying the computational algorithm. However, no details were provided regarding the validation procedure for the proposed methodology. The present work aims to validate and enhance the aforementioned method. For this purpose, a numerical reproduction of an experiment on a submerged U-OWC plant with the same size as the physical one tested by [14] and [41] is conducted, subjecting it to waves with equivalent energy content.

II. The wave-U-OWC interaction

A. Estimation of the captured energy

The evaluation of energy flux captured by a U-OWC plant has been examined through field experiments [14], [41], [42]. This method relies on measuring temperature and pressure fluctuations within the plenum chamber.

Following the procedure described in [14] and [41], three measurement instruments are employed: transducer ① measures water pressure at the upper opening of the vertical duct; transducer ② records pressure in the plenum; and transducer ③ measures air temperature within the plenum (see Fig. 1).

Knowing the pressure inside the plenum, and considering that the air mass in the plenum is constant, the instantaneous volume of the air mass can be evaluated by means of the perfect gas law:

$$p_a V_a = M_a R T_a, \tag{1}$$

and consequently, the free surface displacement ξ, of the water interface in the plenum can be evaluated by means of

$$\frac{\partial \xi}{\partial t} = \frac{1}{A}\frac{\partial V_a}{\partial t}. \tag{2}$$

By applying the continuity equation, the water velocity u_z in the vertical duct can be obtained, which is directly associated to the time derivative of the free surface displacement inside the chamber:

$$u_z = \frac{s''}{s'}\frac{\mathrm{d}\xi}{\mathrm{d}t}, \tag{3}$$

where s' is the width of the vertical duct, and s'', the width of the oscillating water column in the chamber. The energy flux per unit length, captured by the plant can be calculated as:

$$\overline{\Phi}_{abs} = \frac{1}{T}\int_0^T \Delta p(t) u_z(t) s' \mathrm{d}t, \tag{4}$$

where Δp indicates the pressure fluctuations measured by transducer ① at the outer opening of the vertical duct.

B. The 2D numerical experiment

To assess the energy captured by the submerged U-OWC (as depicted in Fig. 1) under wave conditions, a Computational Fluid Dynamics (CFD) simulation was performed. The simulation was conducted within a wave flume, which consists of a piston-type wavemaker positioned at the left end, and a submerged breakwater containing the U-OWC plant at the center. The location of the device was selected to achieve steady-state conditions in the vicinity of the plant for an extended period, while ensuring that the waves radiated from the submerged breakwater do not reflect at the ends of the flume. The wave flume itself is a two-dimensional structure measuring 165 m in length and 4.1 m in height, as illustrated in Fig. 2. The dimensions of the U-OWC breakwater correspond to those described in [41].

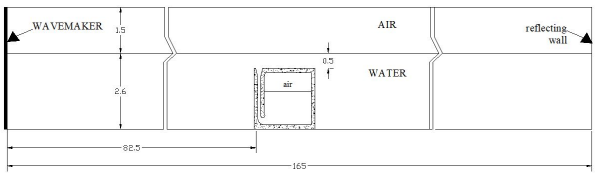

Fig. 2. Sketch of the computational domain and of the U-OWC breakwater.

A hybrid mesh, utilizing the *All Triangle Method* for the overall length of the flume and rectangular elements near the U-OWC device, was employed to discretize the computational domain. The compressible nature of air and the presence of the U-OWC structure led to the implementation of the $k-\omega$ turbulence model in the proximity of the structure.
The wave generation process was simulated by assigning a sinusoidal motion to the left wall of the wave flume using a *User Defined Function* (UDF). The numerical simulation utilized a 2D unsteady Eulerian approach implemented in the commercial software Ansys Fluent v17.0, Academic Version. The water-air interaction was considered using the *Volume of Fluid* (VOF) model. Both fluids were treated as unsteady, and their governing equations, including mass conservation, momentum balance, and energy conservation, were solved. The finite volume method with an implicit formulation in the pressure-based algorithm was employed for the discretization of the governing equations.
To ensure solution convergence and maintain a Courant-Friedrichs-Lewy (CFL) number significantly below 1, a time step $\Delta t = T/1000$ s was employed, where T represents the wave period. For more information about settings of the CFD simulation see [26], [43], [44].

III. Results of the Experiment

A. Performance estimation

The mean energy flux Φ_{abs} absorbed by the plant is determined using Equation (4), which involves integrating the product of Δp and u along the x-direction, at the upper opening of the vertical duct. Fig. 3 illustrates the variations of Δp and the pulsating discharge Q over time. As previously mentioned, U-OWCs exhibit optimal performance when the period of incoming waves matches the eigenperiod of the plant [17].

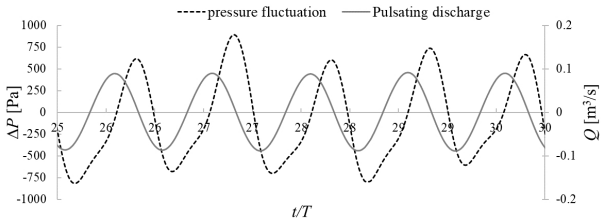

Fig. 3. Pressure fluctuation and pulsating discharge in the vertical duct versus time.

The absorbed energy flux by the U-OWC plant was determined by numerically calculating the elemental flux along a horizontal section of the vertical duct at three points spaced by $\Delta x = 0.03$ m. The evaluation was performed at a distance $z = 0.9$ m, below the still water level and 0.4 m below the upper opening of the U-duct. The results are shown in Fig. 4.

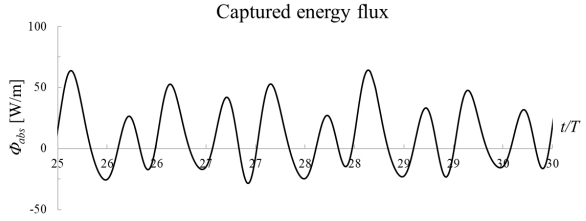

Fig. 4. Energy flux absorbed by the U-OWC plant ($H = 0.1$ m, $T = 2.2$ s).

To assess the impact of the water surface oscillation on the air temperature inside the plenum, six equally

spaced points within the air volume were taken into account, as illustrated in Fig. 5. The analysis of Fig. 5 reveals that the fluctuation of air temperature in the plenum remains independent of spatial position. This is evident from the small percentage difference of approximately 0.1% between the dashed line (T5) and the continuous grey line (T3). Consequently, the choice of measurement location for temperature can be arbitrary. Moving forward, we will refer to the average value of air temperature as T_a. Fig. 6 displays the average temperature and pressure fluctuation inside the air chamber.

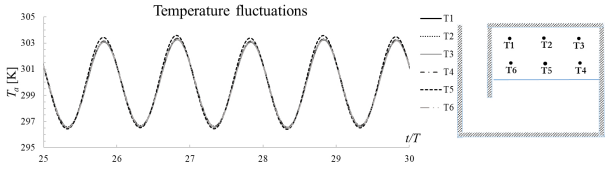

Fig. 5. Fluctuations of the air temperature inside the plenum chamber vs. time.

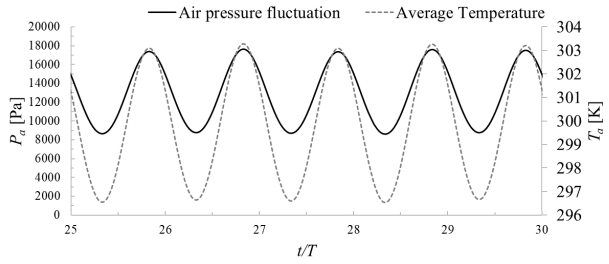

Fig. 6. Fluctuations of the air pressure and of the average air temperature inside the plenum chamber.

Table I shows a summary of the results of the CFD simulations for the wave train simulated.

TABLE I
SUMMARY OF THE RESULTS OF CFD SIMULATIONS

H [m]	T [s]	ξ_0 [m]	ΔT_a [K]	$\overline{\Phi}_{abs}$ [W/m]
0.1	2.2	0.65	6.9	11.21

The performance assessment of a physical plant can be conducted using a 1D mathematical model, where input parameters such as pressure fluctuations at the upper opening of the plant and air pressure/temperature fluctuations within the plenum chamber are considered. The methodology described in Section II-A outlines this approach.

To validate the accuracy of the 1D mathematical model, we employed the results of CFD simulations as input, and compared the outputs of the 1D and 2D models between themselves. Specifically, the pressure fluctuations at the upper opening and the air temperature fluctuations inside the chamber obtained from the 2D simulations were used as input for the 1D model. The variation of air volume in the plenum, and consequently the displacement ξ, were determined using the state law Eq. (1) and Eq. (2).

The comparison between the two curves revealed a very good agreement, indicating the accuracy of the 1D model. This allowed for a precise estimation of the water discharge in the plenum and the U-duct. The evaluation of the absorbed energy flux by integrating the product of water discharge and pressure fluctuation Eq. (4) further confirmed the close agreement between the 1D and 2D models.

Overall, the results demonstrate the reliability and accuracy of the 1D mathematical model in assessing the performance and energy absorption of the plant.

IV. CHARACTERIZATION OF THE THERMAL MEASUREMENT SYSTEM

A. Characterization of the dynamic performances of a thermal gauge

The temperature oscillations in the plenum chamber result from air compression and decompression caused by changes in water level. These oscillations share the same period as the waves interacting with the plant since they are driven by the waves. To design the measurement system, a sensor with a cutoff frequency significantly higher than the maximum frequency in the wind-generated wave bandwidth is needed. It is recommended to choose a sensor with a cutoff frequency at least one decade above. Thermocouples often meet this requirement in their technical specifications, but the declared value corresponds to the intrinsic response time measured in a high thermal capacity medium, according to IEC 60584-2013. However, in actual operating conditions, the time constant of the measurement system will be much higher due to slower heat exchange between the ambient and the thermocouple junction in air compared to contact with liquids or solids.

Expressing the cutoff frequency as

$$\omega_t = \frac{2\pi}{\tau}, \tag{5}$$

it becomes evident that a faster measurement system will have a cutoff frequency further away from the operating frequency.

Increasing the system's speed can be achieved by enhancing heat exchange between the air and the sensor, such as by reducing the junction thickness and improving heat transfer through increased convection. However, these modifications may come with higher costs and reduced system robustness. It's important to note that there is a lower limit for the junction thickness, typically around 0.25 mm, which cannot be exceeded with the current technologies.

Therefore, in order to be able to use the proposed system for the purpose of indirect measurement of the power absorbed by an OWC system, it becomes essential to characterize the measurement system in the operating conditions and specifically, to determine what is the time constant with which the temperature measurement system responds under actual operating conditions.

This involves subjecting the sensor to its intended environment and typical working conditions. In the case of our proposed system, the objective is to characterize a thermal gauge installed in air, considering

various conditions of forced convection in order to improve the sensor performance, by diminishing the response time parameter τ. The most common and straightforward approach to determine τ, is by employing a standard and easily implementable input signal known as a "step signal". By analyzing the output signal of the sensor in response to this input signal, we can obtain the response time τ, using one of the three methods described below.

The first method involves identifying the time instant when the output signal reaches 63.2% of the final steady-state value of the applied step. While this method is simple and practical, it does not guarantee high accuracy. Accurately calculating the value of τ relies on precise knowledge of the moment when the step signal is applied, which may not always be feasible. Uncertainties surrounding this value can introduce errors in determining the time constant.

The second method involves a graphical approach. It entails drawing a tangent line at the beginning of the perturbation on the temperature curve monitored by the sensor, and extending it to the horizontal asymptote representing the final steady-state value. The intersection point of the tangent line and the asymptote corresponds to the time constant. This method offers improved accuracy compared to the first approach, since it considers more data points. However, the reliability of the results obtained using this method is not yet fully guaranteed. The determination of both the zero point and the slope of the curve in the initial phase can be subject to errors [45].

The third method relies on evaluating a linear regression line in logarithmic scale [46]–[49].

Considering that the sensor exhibits first-order dynamics, we can represent the relationship between measured temperature and actual temperature over time:

$$T_m = T_s + (T_f - T_s(1 - e^{-\frac{t}{\tau}}), \tag{6}$$

where T_m represents the measured temperature at time t, T_s represents the actual temperature at the beginning of the measurement interval, and T_f represents the actual temperature at the end of the measurement interval.
Equation 6 can be rearranged as:

$$\frac{T_m - T_f}{T_f - T_s} = e^{-\frac{t}{\tau}}, \tag{7}$$

by introducing a variable $Z(t)$, we can further write

$$Z(t) = \ln \frac{T_m - T_f}{T_f - T_i} = -\frac{T}{\tau}, \tag{8}$$

where he variable Z has the form of a straight line passing through the origin of the axes and with an angular coefficient equal to $-\frac{1}{\tau}$.

The procedure, at this point, is similar to static calibration, involving a linear regression on a set of points to derive an average straight line. The slope of this line represents the response time of the instrument. Two thermal gauges were evaluated: a low-cost 1.5 mm Type J thermocouple with a declared response time (τ) of 0.25 s, and a fast-response 0.25 mm Type K thermocouple, used by Boccotti [14] and Arena and Filianoti [41] in their experiments.

To generate the temperature step, a calibration bath was utilized, and the procedure involved the following steps: inserting the sensor into the calibrator, waiting for the calibrator to reach and stabilize at the target temperature, removing the sensor from the calibrator, and evaluating the step response as it returned to ambient temperature. The ambient temperature was also measured using a PT100 sensor to ensure the attainment of a steady-state condition. To account for the impact of air convection on the thermocouple's time response, four experimental conditions were examined: the sensor placed in still air, the sensor subjected to airflow at velocities of 0.85 m/s, 1.5 m/s, and 2.45 m/s. The airflow was generated using a fan inside a pipe, with its intensity measured by a professional air flow meter. This approach allowed us to evaluate the step response of the sensor and determine the time constant (τ), under different operating conditions and temperature steps, employing Eq. 8. The obtained results are summarized in Table II for the 1.5 mm Type J thermocouple and in Table III for the 0.25 mm Type K thermocouple.

TABLE II
DYNAMIC CHARACTERIZATION IN AIR OF A 1.5 MM TYPE J THERMOCOUPLE AND A 0.25 MM TYPE K THERMOCOUPLE.

Calibrator temperature [°C]	Ambient temperature [°C]	τ [s] - Wind speed 0 m/s	τ [s] - Wind speed 0.85 m/s	τ [s] - Wind speed 1.5 m/s	τ [s] - Wind speed 2.45 m/s
37	17.7	19.7	5.8	5.0	5.3
50	17.7	19.5	5.5	4.3	4.2
60	17.7	20.3	6.0	4.9	4.8
70	17.7	21.0	5.6	5.0	4.7
80	17.7	21.3	5.7	4.8	4.5

TABLE III
DYNAMIC CHARACTERIZATION IN AIR OF A 1.5 MM TYPE J THERMOCOUPLE AND A 0.25 MM TYPE K THERMOCOUPLE.

Calibrator temperature [°C]	Ambient temperature [°C]	τ [s] - Wind speed 0 m/s	τ [s] - Wind speed 0.85 m/s	τ [s] - Wind speed 1.5 m/s	τ [s] - Wind speed 2.45 m/s
37	21.7	12.0	5.0	4.3	4.2
50	21.6	18.0	5.3	4.3	4.0
60	21.6	18.0	5.1	4.3	4.0
70	21.7	17.0	5.0	4.1	3.9
80	21.7	18.2	5.0	4.2	4.4

The differences between the time constants of the two thermocouples are very large in calm air. In this test condition, the thicker thermocouple is almost insensible to the amplitude of the temperature step. On the contrary, the thinner K thermocouple increases its τ by about the 50% in passing the amplitude step from 20 °C to about 60 °C. This increment is due to the high sensitivity of the fast-response thermocouple to even little air flows. The τ of the two thermocouples get smaller in the presence of air convection. From this characterization we can point out that the introduction of a forced convection accelerates the heat exchange

between the sensor and the air, and improves the time response of the measurement system. As we can see, introducing forced convection, the differences between the two systems are strongly reduced, and the time response of the measurement system becomes similar. Considering that the 0.25 mm type K thermocouple used by [14] and [41] in their experiments has considerably higher costs, as well as greater fragility, without bringing substantial benefits compared the cheaper and more robust thermocouple, its use is not advisable, and it can be replaced with a low-cost solution. What remains to be verified at this point is whether the response times of the measurement system are capable of faithfully reproducing the temperature dynamics that typically occur inside the air chamber of a U-OWC. This aspect is discussed in the following.

B. Determination of Time Response Requirements

To achieve indirect flow measurement in OWC systems, where air temperature in the air chamber is used as the measurement parameter, it is crucial to employ a sufficiently fast temperature sensor capable of accurately tracking the rapid temperature changes resulting from the compression and decompression of the air in the plenum.

When considering the actual fluctuations T_{act} of the air temperature in the plenum (i.e., the temperature measured by an ideal gauge) as the input to a practical gauge, as depicted in Fig. 6, the measured temperature T_{meas} will be influenced by the dynamic characteristics of the gauge, including both its amplitude and phase angle. Assuming that the sensor can be mathematically modeled as a first-order instrument, we can express this relationship as follows:

$$a_1 \frac{\mathrm{d}T_{meas}}{\mathrm{d}t} + a_0 T_{meas}(t) = b_0 T_{act}(t), \tag{9}$$

that can be rewritten as:

$$\frac{a_1}{a_0} \frac{\mathrm{d}T_{meas}}{\mathrm{d}t} + T_{meas}(t) = \frac{b_0}{a_0} T_{act}(t), \tag{10}$$

and by defining:

$$\tau \equiv \frac{a_1}{a_0}, \tag{11}$$

$$K \equiv \frac{b_0}{a_0}, \tag{12}$$

we arrive to

$$\tau \frac{\mathrm{d}T_{meas}}{\mathrm{d}t} + T_{meas}(t) = K T_{act}(t). \tag{13}$$

The parameter K represents the system's static sensitivity, indicating the output per unit input for static conditions. Meanwhile, the time constant τ is determined experimentally as the time for the output to reach $63,3\%$ of its final value, after a step change in the input [50]–[52]. Introducing the operational transfer function of the system:

$$\frac{T_{meas}(t)}{T_{act}(t)}(D) = \frac{K}{\tau D + 1}, \tag{14}$$

by utilizing the differential operator D, we can solve the differential equation to obtain the response for any given input. It is crucial to assess how the time response of the temperature gauge influences the evaluation of the plant performance. For this purpose, simulations were conducted using Eq. (14), with K fixed at 1 and applying the input signal $T_{act}(t)$ shown in Fig. 5. The results, summarized in Table IV, provide the relative error between the standard deviations of the input and output signals for different τ values,

$$e_r\% = \frac{|\sigma_{T_{act}} - \sigma_{T_{meas}}|}{\sigma_{T_{act}}}. \tag{15}$$

The graphical results for $\tau = 0.05$ s, 0.5 s and 4.5 s are showed in Fig. 7.

TABLE IV
RELATIVE ERROR BETWEEN STANDARD DEVIATIONS OF THE ACTUAL TEMPERATURE FLUCTUATIONS AND MEASURED ONES, THROUGH A FIRST ORDER INSTRUMENT, HAVING DIFFERENT VALUES OF τ.

$\tau[s]$	e_r [%]
0.01	0
0.05	0.3
0.1	0.9
0.2	3.2
0.3	6.7
0.4	11
0.5	15.7
1	37.5
2	59.8
4.5	70.9

For values of τ less than or equal to 0.1s, the sensor demonstrates highly accurate reproduction of temperature variations over time, with an accuracy exceeding 99%. However, as τ increases, the performance of the sensor deteriorates, ultimately losing its ability to track temperature fluctuations entirely when τ approaches the period of oscillation of the air temperature (refer to Fig. 7c). In the subsequent section, we assess the impact of temperature measurement errors on the measurement of captured power by the OWC system.

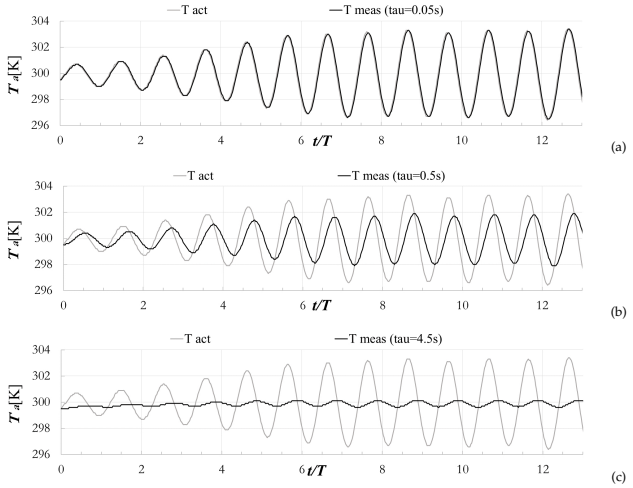

Fig. 7. Simulation of a first order response – temperature trend a) $\tau = 0.05$ s, b) $\tau = 0.5$ s, c) $\tau = 4.5$ s.

As the reader can see, as the time constant τ increases, the amplitude of the temperature fluctuations become smaller and the time shift, larger. For $\tau = 0.5$ s, the amplitude of T_{meas} is halved compared to the actual one, T_{act}. The phase shift passes from zero, for

$\tau = 0.01$ s to 109 degree, for $\tau = 0.5$ s. Following the procedure described in Sect. II-A, considering as input the temperature signals obtained from the thermocouple simulations, we calculated the energy flux captured by the plant, which is shown in Fig. 8. For comparison, the energy flux obtained by means of the CFD simulation is also shown.

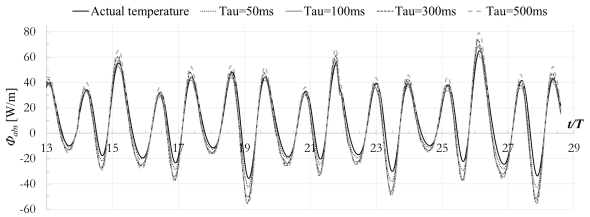

Fig. 8. Energy flux captured by the U-OWC plant: comparison between 2D model (actual temperature) and the results of the 1D model, obtained using as input the different temperature histories obtained as output of the first order system, using different values of τ.

Table V provides a summary of the simulation results, focusing on the estimation error e_r for the captured energy flux Φ_{abs} by the plant. This error is influenced by two factors: the reduction in temperature amplitude and the phase angle shift. Interestingly, these factors have opposite effects on the energy flux estimation.

A decrease in temperature amplitude increases the captured energy flux. Conversely, an increase in the phase angle shift leads to a reduction in the energy flux. These observations are consistent with the results in Table V, where increasing τ results in smaller flux estimations and higher errors, reaching a maximum of 46% at $\tau = 0.1$ s.

As τ further increases, the flux estimation grows, while the relative error decreases. This is primarily due to the dominant role of reduced temperature fluctuation amplitude.

TABLE V
SUMMARY OF THE SIMULATION FOR DIFFERENT VALUES OF τ.

τ [s]	T_{max} [K]	T_{min} [K]	ϵ [rad]	$\overline{\Phi}_{abs}$ [kW/m]	$e_r(\overline{\Phi}_{abs})$ [%]
0.01	303.4	296.4	0	8.2	21
0.05	303.4	296.5	0.31	7.1	32
0.1	302.9	296.9	1.26	5.6	46
0.3	302.5	297.2	1.57	6.1	41
0.5	301.9	297.9	1.9	7.9	23
1.0	301.0	298.7	2.8	10.9	6

V. CONCLUSIONS

The measurement of captured power is critical for assessing the performance of an energy conversion system. In the case of a U-OWC wave energy converter, traditionally, water velocity measurement in the U-duct is used. However, an alternative method proposed by Boccotti [14] and Arena and Filianoti [41] suggests measuring air temperature fluctuations in the plenum instead. In this study, we analyze the influence of the time response of a thermocouple on the measurement of captured energy flux.

To this aim, we replicate a numerical experiment of a submerged U-OWC system described by Arena and Filianoti [41], aiming to accurately reproduce the system's dynamic behavior.

We described a methodology to estimate the time response of a thermal gauge subjected to air ventilation, as done during the experiments by [41].

Assuming a first-order behavior for the temperature sensor, we evaluate the captured energy fluxes by varying the time response. The estimation error of the energy flux is analyzed in terms of amplitude damping and phase angle shift. Specifically, reducing the amplitude of the measured temperature fluctuation leads to an overestimate of the energy flux, while a forward shift in the phase angle underestimates the energy flux. The results indicate that, recurring to forced ventilation is not enough to achieve a precise estimation of the wave power captured by the plant. Some adaptive correction of thermal measurements could reach the scope.

REFERENCES

[1] Fulco G., Ruffa F., Lugarà M., Filianoti P., De Capua C., "Automatic station for monitoring a microgrid", in Proceedings of the 24th IMEKO TC4 International Symposium and 22nd International Workshop on ADC and DAC Modelling and Testing, 2022, September, Palermo, Italy (pp. 14-16).

[2] Czech B. and Bauer P., "Wave Energy Converter Concepts: Design Challenges and Classification" in IEEE Industrial Electronics Magazine, vol. 6, no. 2, pp. 4-16, June 2012, doi: 10.1109/MIE.2012.2193290.

[3] López I., Andreu J., Ceballos S., Martínez de Alegría I., Kortabarria I., "Review of wave energy technologies and the necessary power-equipment", Renewable and Sustainable Energy Reviews, Vol. 27, pp. 413-434,2013. https://doi.org/10.1016/j.rser.2013.07.009

[4] Drew B., Plummer A.R., Sahinkaya M.N., "A review of wave energy converter technology", Proceedings of the Institution of Mechanical Engineers, Part A: Journal of Power and Energy. 2009;223(8):887-902. doi:10.1243/09576509JPE782

[5] Heath T. V., "A review of oscillating water columns", Phil. Trans. R. Soc., Vol. 370, pp 235–245, 2012.

[6] Falcão A.F.O., "Wave energy utilization: A review of the technologies", Renewable and Sustainable Energy Reviews, Vol. 14, Issue 3, pp. 899-918, 2010. https://doi.org/10.1016/j.rser.2009.11.003

[7] Benreguig P., Kelly J., Pakrashi V., Murphy J., "Wave-to-Wire Model Development and Validation for Two OWC Type Wave Energy Converters", Energies. 12(20):3977, 2019. https://doi.org/10.3390/en12203977

[8] Falcão A.F.O., Henriques J.C.C., "Oscillating-water-column wave energy converters and air turbines: A review", Renewable Energy, Vol. 85, 2016, pp. 1391-1424, ISSN 0960-1481. https://doi.org/10.1016/j.renene.2015.07.086

[9] Falcão A.F.O., "The shoreline OWC wave power plant at the Azores", in Proc 4th European Wave Energy Conf, Aalborg, Denmark, pp. 42-47, 2000.

[10] Heath T., Whittaker T.J.T., Boake C.B., "The design, construction and operation of the LIMPET wave energy converter (Islay, Scotland)", in Proc. 4th European Wave Energy Conf, Aalborg, Denmark, pp. 49-55, 2000.

[11] Suzuki M., Arakawa C., Takahashi S., "Performance of wave power generating system installed in breakwater at Sakata port in Japan", in Proc. 14th Int Offshore Polar Eng Conf, Toulon, France, pp. 202-209, 2004.

[12] Heath T.V., "The development of a turbo-generation system for application in OWC breakwaters", in Proc. 7th European Wave Tidal Energy Conf, Porto, Portugal, 2007.

[13] Washio Y., Osawa H., Nagata Y., Fujii F., Furuyama H., Fujita T., "The offshore floating type wave power device "Mighty Whale": open sea tests", in Proc. 10th Int Offshore Polar Eng Conf, Seattle, vol. 1, pp. 373-380, 2000.

[14] Boccotti P.,"On a new wave energy absorber" Ocean Engineering 30(9), pp. 1191-1200, 2003.

[15] Boccotti P., "Caisson breakwaters embodying an OWC with a small opening - Part I: Theory", Ocean Engineering 34 (5-6), 806-819 2007.

[16] Boccotti P., "Design of breakwater for conversion of wave energy into electrical energy", Ocean Engineering, Volume 51, 1 September 2012, Pages 106-118, 2012.

[17] Boccotti P. , "Wave mechanics and wave loads on marine structure", Amsterdam; Boston, Butterworth-Heinemann, an imprint of Elsevier, 2015.

[18] Boccotti P. , Filianoti P.G.F., Fiamma V., Arena F., "Caisson breakwaters embodying an OWC with a small opening - Part II: A small-scale field experiment", Ocean Engineering 34 (5-6), 820-841, 2007.

[19] Caprara G. , Martirano L. , Kermani M., de Mesquita e Sousa D., Barilli R., Armas V. , "Cold Ironing and Battery Energy Storage System in the Port of Civitavecchia," 2022 IEEE International Conference on Environment and Electrical Engineering and 2022 IEEE Industrial and Commercial Power Systems Europe (EEEIC / I&CPS Europe), 2022, pp. 1-6. https://doi.org/10.1109/EEEIC/ICPSEurope54979.2022.9854593

[20] Filianoti P., Piscopo R., "Sea wave energy transmission behind submerged absorber caissons", Ocean Engineering, Vol. 93, pp. 107-117, 2015. https://doi.org/10.1016/j.oceaneng.2014.09.031

[21] Hsien Hua Lee, Chen-Yen Wen and Guan-Fu Chen, "Study on an Oscillating Water Column Wave Power Converter Installed in an Offshore Jacket Foundation for Wind-Turbine System Part II: Experimental Test on the Converting Efficiency", Processes 2022,10, 418. https://doi.org/10.3390/pr10020418

[22] M'zoughi F., Garrido I., Garrido A.J., De La Sen M, "Rotational Speed Control Using ANN-Based MPPT for OWC Based on Surface Elevation Measurements", Appl. Sci. 2020, 10, 8975. https://doi.org/10.3390/app10248975

[23] Ceballos S., Rea J., Robles E., Lopez I., Pou J., O'Sullivan D., "Control Strategies for Combining Local Energy Storage with Wells Turbine Oscillating Water Column Devices", Renewable Energy, Volume 83, 2015, Pages 1097-1109, ISSN 0960-1481, https://doi.org/10.1016/j.renene.2015.05.030.

[24] Faÿ F.X., Pujana A., Ruiz-Minguela P., Kelly J., Mueller M., Henriques J., Gato L., Carrelhas A., Lopes B., Aldaiturriaga E., "Shoreline OWC wave power plant control algorithms" OPERA Project Deliverable, Grant Agreement No 654444

[25] Kooverji B., "Pneumatic Power Measurement of an Oscillating Water Column Converter", Dissertation presented for the degree of Master of Science in Engineering (Mechatronic) in the Faculty of Engineering, 2014, Stellenbosch University

[26] Gurnari L., Filianoti P.G.F., Torresi M., Camporeale S.M., "The wave-to-wire energy conversion process for a fixed U-OWC device", Energies, 2020, 13(1), 283.

[27] Benreguig P., Pakrashi V., Murphy J., "Assessment of Primary Energy Conversion of a Closed-Circuit OWC Wave Energy Converter", Energies 2019, doi:10.3390/en12101962.

[28] Suchitra R., Ezhilsabareesh K., Samad A., "Development of a reduced order wave to wire model of an OWC wave energy converter for control system analysis", Ocean Eng. 2019, 172, 614–628.

[29] Ciappi L., Cheli L., Simonetti I., Bianchini A., Talluri L., Cappietti L., Manfrida G., "Analytical Models of Oscillating Water Column Systems Operating with Air Turbines in the Mediterranean Sea", in Proceedings of the 15th Conference on Sustainable Development of Energy, Water and Environment Systems, Cologne, Germany, 1–5 September 2020.

[30] Mayon R., Ning D., Zhang C., Chen L., Wang R., "Wave energy capture by an omnidirectional point sink oscillating water column system", Applied Energy, Volume 304, 2021, 117795, ISSN 0306-2619, https://doi.org/10.1016/j.apenergy.2021.117795.

[31] Cappietti L., Simonetti I., Penchev V., Penchev P., "Laboratory tests on an original wave energy converter combining oscillating water column and overtopping devices", Advances in Renewable Energies Offshore – Guedes Soares (ed.) © 2019 Taylor & Francis Group, London, ISBN 978-1-138-58535-5.

[32] Pereira T.S.R., de Carvalho T.P., Mendes T.A., Formiga K.T.M., "Evaluation of Water Level in Flowing Channels Using Ultrasonic Sensors", Sustainability 2022, 14, 5512. https://doi.org/10.3390/su14095512

[33] David D.R., Sundar V., Sannasiraj S.A., "Optmizing the opening angle of the harbour wall in an oscillating water column", HYDRO 2016 INTERNATIONAL-21st International Conference on hydraulics, Water Resources and Coastal Engineering 8-10 Dec 2016 Pune, India.

[34] Filianoti P., "Pulsating flow discharge measurements inside a wave energy converter at sea", Proceedings of the 6th IMEKO TC19 Symposium on Environmental Instrumentation and Measurements, Reggio Calabria, Italy, 2016.

[35] Shalby M., Elhanafi A., Walker P., Dorrell D.G., "CFD modelling of a small–scale fixed multi–chamber OWC device", Applied Ocean Research,Volume 88, 2019, Pages 37-47, ISSN 0141-1187, https://doi.org/10.1016/j.apor.2019.04.003.

[36] Weber J., "Representation of non-linear aero-thermodynamic effects during small scale physical modelling of Oscillating Water Column wave energy converters", Seventh European Wave and Tidal Energy Conference, January 2007,Porto, Portugal.

[37] Gomes R.P.F. , Henriques J.C.C. , Gato L.M.C., Falcão A.F.O., "Testing of a small-scale floating OWC model in a wave flume", 4th International Conference on Ocean Energy, 17 October, Dublin.

[38] Gomes R.P.F, Henriques J.C.C., Gato L.M.C., Falcao A.F.O., "Testing of a small-scale floating OWC mode in a wave channel and comparison wit numerical results", Renewable Energies Offshore – Guedes Soares (Ed.), 2015, Taylor & Francis Group, London, ISBN 978-1-138-02871.

[39] Filianoti P., Camporeale S., "In Field Measurements On A Small Scale OWC Device", Proceedings of the 8th European Wave and Tidal Energy Conference, Uppsala, Sweden, 7-10 September 2009, ISSN 2309-1983.

[40] Shalby M., Elhanafi A., Walker P. et al., "Experimental Investigation of the Small-scale Fixed Multi-chamber OWC Device", Chin. J. Mech. Eng. 34, 124 (2021). https://doi.org/10.1186/s10033-021-00641-9

[41] Arena F., Filianoti P.,"Small-scale field experiment on a submerged breakwater for absorbing wave energy", Journal of Waterway, Port, Coastal and Ocean Engineering, 2007, 133(2), pp. 161–167.

[42] Filianoti P., Camporeale S.M., "A linearized model for estimating the performance of submerged resonant wave energy converters", Renewable Energy Volume 33, Issue 4, April 2008, Pages 631-641 (2008).

[43] Gurnari L., Filianoti P.G.F., Camporeale S.M., "Fluid dynamics inside a U-shaped oscillating water column (OWC): 1D vs. 2D CFD model", Renewable Energy, 2022, 193, pp. 687–705.

[44] Filianoti P., Gurnari L., "The performance of an "active" submerged breakwater by a cfd analysis", Proceedings of the International Offshore and Polar Engineering Conference, 2019, 3, pp. 3702–3705.

[45] Niemann H., Miklos R., "A Simple Method for Estimation of Parameters in First order Systems", Journal of Physics: Conference Series, Vol. 570, no.1, 2014.

[46] Doebelin E.O., "System Dynamics: Modeling, Analysis, Simulation, Design", Dekker: NY, 1998.

[47] Doebelin E.O., "Measurement Systems", 4/e, McGraw-Hill: NY, 1990.

[48] Incropera F.P., DeWitt D.P., "Introduction to Heat Transfer", Wiley: NY, 1985.

[49] Wheeler A.J., Ganji, A.R., "Introduction to Engineering Experimentation", Prentice Hall: Upper Saddle River, NJ, 1996.

[50] R.P. Benedict, "Fundamentals of temperature, pressure, and flow measurements – 3rd edition", John Wiley & Sons, New York, 1984.

[51] McGee T.D., "Principles and methods of temperature measurements", John Wiley & Sons, New York, 1988.

[52] Kerlin T.W., "Industrial Temperature Measurement", Instrument Society of America, Research Triangle Park, N.C., 1982.